Development 136, 4225-4233 (2009) doi:10.1242/dev.036723

Indirect modulation of Shh signaling by Dlx5 affects the oral-nasal patterning of palate and rescues cleft palate in *Msx1*-null mice

Jun Han[1], Julie Mayo[1], Xun Xu[1], Jingyuan Li[1], Pablo Bringas, Jr [1], Richard L. Maas[2], John L. R. Rubenstein[3] and Yang Chai[1,*]

Cleft palate represents one of the most common congenital birth defects in human. During embryonic development, palatal shelves display oronasal (O-N) and anteroposterior polarity before the onset of fusion, but how the O-N pattern is established and how it relates to the expansion and fusion of the palatal shelves are unknown. Here we address these questions and show that O-N patterning is associated with the expansion and fusion of the palatal shelves and that *Dlx5* is required for the O-N patterning of palatal mesenchyme. Loss of *Dlx5* results in downregulation of *Fgf7* and expanded *Shh* expression from the oral to the nasal side of the palatal shelf. This expanded Shh signaling is sufficient to restore palatal expansion and fusion in mice with compromised palatal mesenchymal cell proliferation, such as *Msx1*-null mutants. Exogenous Fgf7 inhibits Shh signaling and reverses the cranial neural crest (CNC) cell proliferation rescue in the *Msx1*/*Dlx5* double knockout palatal mesenchyme. Thus, Dlx5-regulated Fgf7 signaling inhibits the expression of Shh, which in turn controls the fate of CNC cells through tissue-tissue interaction and plays a crucial role during palatogenesis. Our study shows that modulation of Shh signaling may be useful as a potential therapeutic approach for rescuing cleft palate.

KEY WORDS: Msx1, Dlx5, Cranial neural crest (CNC) cells, Palate, Shh

INTRODUCTION

Cleft palate represents one of the major groups of congenital birth defects in the human population. Despite recent advancements in medical intervention, babies born with cleft palate often suffer multiple handicaps that significantly compromise the quality of their lives. The mammalian palate develops from two primordia: the primary palate and the secondary palate. The primary palate represents only a small part of the adult hard palate. The secondary palate is the primordium for most of the hard and all of the soft parts of the palate. Palate development is a multistep process that involves palatal shelf growth, elevation, midline fusion of palatal shelves and the disappearance of the midline epithelial seam. The palatal structures are composed of the cranial neural crest (CNC)-derived ectomesenchyme and pharyngeal ectoderm (Ferguson, 1988; Shuler, 1995). Throughout palatal development, there is continuous epithelial-mesenchymal interaction that is essential for the growth and fusion of the palate. The most common type of cleft palate documented in animal studies, which also most closely resembles cleft palate in humans, is the failure of palate shelf expansion following elevation (Chai and Maxson, 2006; Ito et al., 2003; Rice et al., 2004; Satokata and Maas, 1994).

In the developing palate, the epithelia that cover the palatal shelves are divided into oral, nasal and medial edge epithelium (Chai and Maxson, 2006). The nasal and oral epithelia differentiate into pseudostratified and squamous epithelia, respectively, whereas the medial edge epithelium (MEE) is removed from the fusion line by means of programmed cell death and cell migration (Martinez-Alvarez et al., 2000; Vaziri Sani et al., 2005). The palatal mesenchyme is mainly derived from CNC cells (Ito et al., 2003) and has been treated as a homogeneous population in previous studies. The oral-nasal patterning of the palatal mesenchyme and the molecular regulation of the fate of mesenchymal cells must be taken into account when analyzing palatal development.

Dlx5, Shh and Msx1 control the fate of CNC cells. Specifically, Dlx5 plays a critical role in regulating the patterning of craniofacial structures (Depew et al., 1999; Qiu et al., 1997; Yang et al., 1998). Nested *Dlx* gene expression in the branchial arches patterns proximodistal axes and is crucial in the acquisition and refinement of mammalian jaws through evolution (Depew et al., 2002). Sonic hedgehog (Shh) mediates the ventral inductive signaling during the dorsoventral patterning of the spinal cord (Jessell, 2000). Within the CNC population, Shh is required for cardiac outflow tract and facial primordial development via regulation of CNC cell survival and proliferation (Jeong et al., 2004; Washington Smoak et al., 2005). During palatogenesis, *Shh* expression is restricted to the oral side of the palatal epithelium, and conditional inactivation of *Shh* in the ectoderm leads to dramatic shortening of the palatal shelves and cleft palate (Lan and Jiang, 2009; Rice et al., 2004). Exogenous Shh stimulates palatal mesenchyme proliferation in palatal explant culture (Bei et al., 2000). Interestingly, a recent study shows that overexpression of Shh signaling in the palatal ectoderm also leads to cleft palate (Cobourne et al., 2009). Collectively, these studies suggest that Shh signaling needs to be tightly regulated during palatogenesis.

Msx1 is crucial for the development of palate, teeth and other craniofacial structures (Han et al., 2003; Satokata and Maas, 1994). In humans, mutations in the *MSX1* gene result in orofacial clefting and tooth agenesis, consistent with the phenotype observed in *Msx1*

[1]Center for Craniofacial Molecular Biology School of Dentistry University of Southern California, 2250 Alcazar Street, CSA 103, Los Angeles, CA 90033, USA. [2]Genetics Division, Department of Medicine, Brigham and Women's Hospital and Harvard Medical School, Boston, MA 02115, USA. [3]Nina Ireland Laboratory of Developmental Neurobiology, University of California San Francisco, Genetics and Development, San Francisco, CA 94158, USA.

*Author for correspondence (ychai@usc.edu)

Accepted 5 October 2009

mutant mice (Hu et al., 1998; Jumlongras et al., 2001; van den Boogaard et al., 2000; Vastardis et al., 1996). In mice, Msx1 is required for *Bmp4* and *Bmp2* expression in the palatal mesenchyme and *Shh* expression in the palatal epithelium. Shh acts downstream of Bmp4 and upstream of Bmp2 to stimulate mesenchymal cell proliferation to promote the outgrowth of the palatal shelf (Zhang et al., 2002).

We have investigated the establishment of O-N patterning in the palate by assaying the expression of various asymmetric gene markers and investigating the palatal phenotype associated with the loss of *Dlx5* in mice. We find that oronasal (O-N) patterning is associated with the expansion and fusion of the palatal shelves and that *Dlx5* is required in the O-N patterning of palatal mesenchyme. *Dlx5* is specifically required for *Fgf7* expression in the nasal side of palatal mesenchyme. Furthermore, Fgf7 strongly inhibits *Shh* expression in the nasal side of palatal shelf epithelium. Loss of *Dlx5* results in downregulation of *Fgf7* and an expansion of *Shh* expression into the nasal side of the palatal epithelium. This expanded Shh signaling is sufficient to rescue palatal fusion, as *Msx1/Dlx5* double-null mutant mice show restored CNC cell proliferation and palate fusion. Furthermore, Msx1 and Dlx5 antagonistically regulate the expression of *Shh*, which in turn controls the fate of CNC cells through tissue-tissue interaction during palatogenesis. Finally, we report that Dlx5 is crucial for the patterning of soft palate.

MATERIALS AND METHODS

Mutant mice, histological and skeleton analysis and scanning electron microscopy (SEM)

Mice carrying *Msx1*$^{+/-}$ and *Dlx5*$^{+/-}$ alleles have been described previously (Depew et al., 1999; Satokata and Maas, 1994). We crossed *Msx1*$^{+/-}$*; Dlx5*$^{+/-}$ mice to generate *Msx1/Dlx5* double-null mutants. All samples were fixed in 10% buffered formalin and processed through serial ethanol, and paraffin embedded and sectioned using routine procedures. For general morphology, deparaffinized sections were stained with Hematoxylin and Eosin (H and E) using standard procedures. Skeletal structures were stained using Alcian Blue for non-mineralized cartilage and Alizarin Red for bone, as described previously (Ito et al., 2003). For SEM, samples were fixed with 10% buffered formalin at 4°C overnight. After dehydration through a graded ethanol series, samples were trimmed and dried in a Balzer Union (FL-9496) apparatus, and coated with colloidal silver liquid (Ted Pella) by a Technics Hummer V Sputter Coater. Samples were examined with a Cambridge 360 scanning electron microscope.

Palatal shelf organ cultures and bead implantation

Timed-pregnant mice were killed on post-coital day 13.5 (E13.5). Genotyping was carried out as previously described (Depew et al., 1999; Satokata and Maas, 1994). Paired secondary palatal shelves were microdissected and cultured in serumless, chemically defined medium as previously described (Ito et al., 2003). For bead implantation, Affi-Gel blue agarose beads (BioRad) were soaked in proteins as previously described (Zhang et al., 2002). Tissues were harvested after 24 hours of culture and fixed in 4% paraformaldehyde for processing. Shh N-terminal peptide (R&D Systems) was used at 1 mg/ml, anti-Shh antibody (Developmental Studies Hybridoma Bank) was used at 0.30 mg/ml and BSA was used at 10 ng/ml. Neutralizing antibodies to Fgf7 (MAB251) and Mouse IgG1 (MAB002) (R&D Systems) were added to the culture medium at concentrations of 50 μg/ml.

Apoptosis and cell proliferation

Following treatment with 20 mg/ml proteinase K for 15 minutes at room temperature, apoptotic cells were assayed by the TUNEL procedure using the In Situ Cell Death Detection Kit, Fluorescein (Roche Molecular Biochemicals) by following the manufacturer's protocol. Cell proliferation was scored by injection of 5-bromo-2′-deoxyuridine (BrdU, Sigma, 100 μg/g body weight) into pregnant females 1 hour before recovery of embryos. For palatal organ culture, BrdU was supplemented into culture medium at concentration of 100 μM for 2 hours before harvest. Detection of BrdU-labeled cells was carried out using a BrdU Labeling and Detection Kit following the manufacturer's protocol (Zymed).

In situ hybridization

Samples for whole-mount and section in situ hybridization were fixed in freshly made 4% paraformaldehyde/PBS. In situ hybridizations were performed as previously described (Xu et al., 2005). The following cDNAs were used to generate antisense riboprobes: a 1.2 kb fragment of mouse *Msx1*, a 900 bp mouse *Dlx5*, a 1.6 kb mouse *Gli1* and 640 bp mouse *Shh*. Non-radioactive RNA probes were generated by in vitro transcription labeling with digoxigenin-UTP according to the manufacturer's protocol (Roche Molecular Biochemicals).

Real-time PCR

E13.5 palatal shelves (six wild type and six mutants, in two independent experiments) were precisely dissected. Total RNA was extracted using the RNeasy Kit (Qiagen, USA). Quality of RNA, primer efficiency and correct size were tested by RT-PCR. Real-time PCR was performed with Cycler (Bio-Rad) using iQ SYBR Green (Bio-Rad). 18S RNA was used to normalization.

Primer sequences are: 18S, 5′-CGGCTACCACATCCAAGGAA-3′; 18S AS, 5′-GCTGGAATTACCGCGGCT-3′; Fgf7 F, 5′-CTCTACAGGTC-ATGCTTCCACC-3′; Fgf7 R, 5′-ACAGAACAGTCTTCTCACCCT-3′.

RESULTS

Oronasal patterning of mouse palatal mesenchyme

The palatal epithelia is heterogeneous in newborn mice, with pseudostratified, ciliated, columnar epithelia covering the nasal side of the palatal shelf and stratified keratinizing, squamous epithelia covering the oral side (Fig. 1A,B). Mesenchymal heterogeneity of the nasal and oral regions of the palate is subtle, with the palatine bone in the nasal region and soft tissue in the oral region (Fig. 1B). We hypothesized that these morphological differences are likely to be the result of molecular heterogeneity established earlier along the oronasal (O-N) axis of developing palate. In fact, *Dlx5*, *Fgf7* and phospho-Smad1/5/8 expression is restricted to the nasal region at E13.5 (Fig. 1C-F), whereas *Gli1* and *Fgf10* are expressed mainly in the oral region of the palatal mesenchyme (Fig. 1H-K). *Shh* is expressed only in the oral side of palatal epithelium at E13.5 (Fig. 1G).

Inactivation of *Dlx5* leads to an expansion of the oral region of the palatal shelf

Previous studies examining *Dlx5*$^{-/-}$ mice were based on skeletal staining, which revealed incomplete palatal bone fusion (Depew et al., 1999; Levi et al., 2006). In order to characterize the palatal phenotype thoroughly, we performed scanning electron microscopy (SEM) on *Dlx5*$^{-/-}$ mice. In the anterior region of the palate, the soft tissue was fused in all *Dlx5*$^{-/-}$ mice (n=45) (Fig. 2A-D). Although some *Dlx5*$^{-/-}$ mice (n=5, 11%) were born with a groove (a folding of the palatal shelf) in the palate (Fig. 2C), histological analysis clearly revealed that there was normal soft tissue connection between the two palatal shelves (Fig. 2D). The landmark of the oral palatal epithelium, the rugae, are detectable in SEM images of the oral side of newborn palatal shelves (Fig. 2A,B, white arrows). Compared with wild-type littermates, the rugae in *Dlx5*$^{-/-}$ mice appear more prominent, both in the SEM image (Fig. 2A,B) and the H and E staining of sagittal sections through the rugae (Fig. 2E,F). We detected approximately a 40% increase in the height of the ruga and 40% increase in the thickness of the squamous epithelium in *Dlx5*$^{-/-}$ mutants relative to wild type (Fig. 2F). We did not detect any

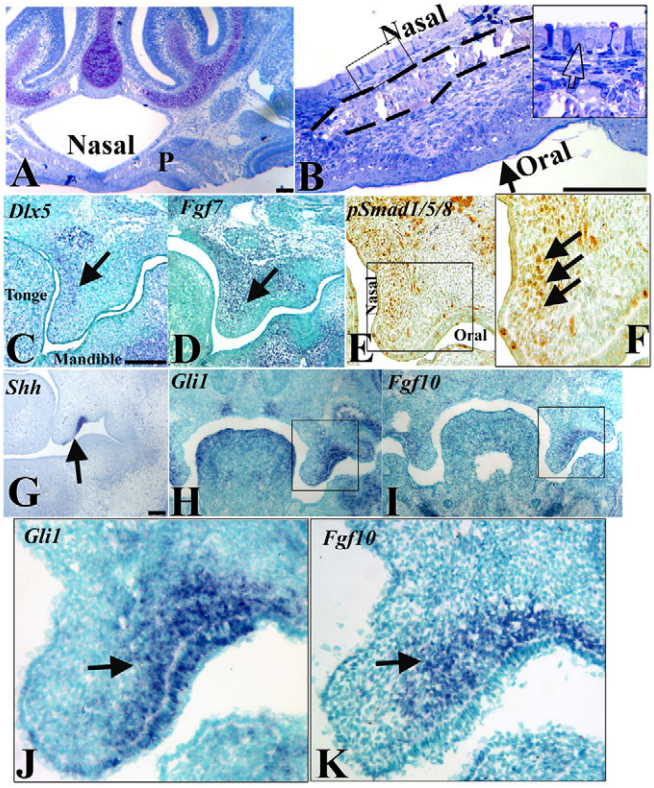

Fig. 1. Oronasal patterning of the palate. (**A**,**B**) Toluidine Blue staining of semi-thin sections of newborn head showing regional morphology of the palatal epithelium of wild-type mice: a coronal section of the palate (A) and an enlarged palatal shelf (B). The box in B is enlarged in the insert, and shows pseudostratified, ciliated, columnar epithelia that cover the nasal side of the palatal shelf. Broken lines outline the palatal bone. (**C-F**) Expression of nasal side markers in coronal sections of the palate at E13.5 assayed by ISH for *Dlx5* (C) and *Fgf7* (D) and immunostaining of phospho-Smad1/5/8 (E,F). F is enlarged from the box in E. (**G-K**) Expression of oral side markers in coronal sections of the palate at E13.5 assayed by in situ hybridization of *Shh* (G), *Gli1* (H,J) and *Fgf10* (I,K). J and K are enlargements of boxes in H and I, respectively. Scale bars: 200 μm.

difference in stratification of the oral side of the palatal epithelium in *Dlx5*$^{-/-}$ mutants. By contrast, the thickness of the nasal side palatal epithelium in *Dlx5*$^{-/-}$ mice is comparable to that of the wild-type control (see Fig. S1 in the supplementary material). The expansion of the oral side of the palate shelf is most obvious in *Dlx5*$^{-/-}$ mutants with excencephaly (representing 11% of *Dlx5*$^{-/-}$ mice), in which the oral palatal epithelium protrudes into the palate forming a groove (Fig. 2C). The expansion of the oral side of the palate shelf in *Dlx5*$^{-/-}$ mice can be detected at E13.5 based on the expansion of *Shh* expression into the MEE and nasal side of the palatal epithelium (Fig. 2I-L). This is an expansion, not a shift, as the oral side *Shh* expression persists (Fig. 2J). In wild-type mice, *Shh* is not expressed in the MEE and nasal side of the palatal epithelium. We confirmed previous studies that reported diminished *Shh* expression in the anterior part of the oral palatal epithelium in *Msx1*$^{-/-}$ mutant mice (Fig. 2O) (Zhang et al., 2002). We also found that the expression of *Gli1*, a key hedgehog (Hh) pathway target (Hooper and Scott, 2005; Lum and Beachy, 2004), expanded from the oral region of the palate into the nasal region in *Dlx5*$^{-/-}$ mice (Fig. 3A,B). Phospho-Smad1/5/8, and *Fgf7* were detectable in the nasal region of the palatal mesenchyme in wild-type mice, but their expression was reduced in *Dlx5*$^{-/-}$ mutants (Fig. 3D,E,G,H,J). Our quantitative PCR

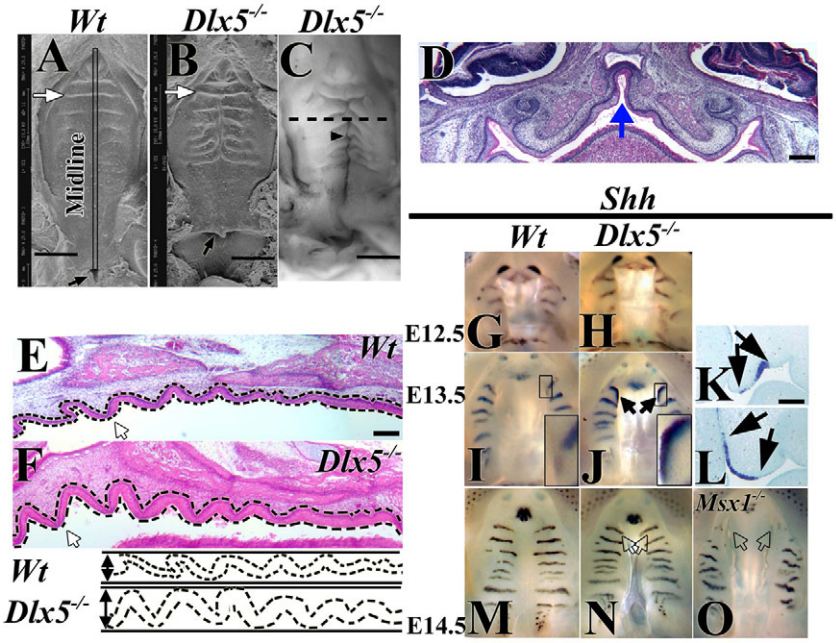

Fig. 2. Excessive growth of the oral side of the palate in *Dlx5*$^{-/-}$ mice. (**A-C**) Scanning electron microscopy (SEM) of newborn wild-type and *Dlx5*$^{-/-}$ mice heads (oral view). Some (11%) *Dlx5*$^{-/-}$ mice have a groove in the hard palate (C). Vertical line: the fusion midline of palatal shelves (A). Black arrow: posterior edge of soft palate (A,B). White arrow: rugae (A,B). Arrowhead: folding of the palate shelf (C). Broken line (C): the plane of the section shown in D. (**D**) H and E staining of coronal section of the *Dlx5*$^{-/-}$ newborn head in C. (**E**,**F**) H and E staining of sagittal sections of newborn head. White arrow: rugae (E,F). Broken lines (below F): trace of the oral epithelium. (**G-O**) Whole-mount and section in situ hybridization (ISH) of *Shh* in oral epithelium at E12.5 (G,H), E13.5 (I-L) and E14.5 (M-O) in wild-type and *Dlx5*$^{-/-}$ mice. Arrows: the expression domain of *Shh* in the palatal epithelium (I-L). Inserts are the enlarged boxed areas in I and J. Whole-mount ISH of *Shh* in palatal epithelium at E14.5 also includes *Msx1*$^{-/-}$ mice (M-O). Open arrows: expanded *Shh* expression in *Dlx5*$^{-/-}$ mice (N) and diminished *Shh* expression in *Msx1*$^{-/-}$ mice (O). Scale bar: 1 mm in A-C; 200 μm in E-L.

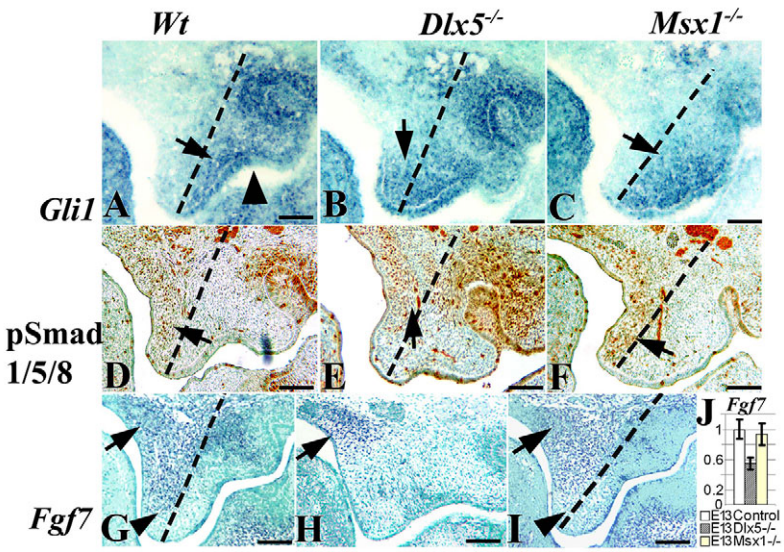

Fig. 3. Altered oronasal patterning in *Dlx5*$^{-/-}$ palate. (**A-C**) In situ hybridization (ISH) of *Gli1* in coronal sections of E13.5 wild type (A, arrowhead indicates the anteroposterior groove between the palatal process and the body of the maxilla), *Dlx5*$^{-/-}$ (B), and *Msx1*$^{-/-}$ palate (C). (**D-F**) Immunostaining of phospho-Smad1/5/8 in coronal sections of E13.5 wild-type (D), *Dlx5*$^{-/-}$ (E) and *Msx1*$^{-/-}$ palate (F). (**G-I**) ISH of *Fgf7* in coronal sections of E13.5 wild-type (G), *Dlx5*$^{-/-}$ (H), and *Msx1*$^{-/-}$ palate (I). (**J**) Real-time PCR quantification of *Fgf7* mRNA abundance in *wild type*, *Dlx5*$^{-/-}$ and *Msx1*$^{-/-}$ palatal tissue. Arrows and arrowheads: the expression domains of *Fgf7*. Dashed lines divide palatal shelves into nasal and oral domains. Scale bars: 200 μm.

analysis confirmed greater than 40% reduction in *Fgf7* expression in the palate of *Dlx5*$^{-/-}$ mice (Fig. 3J). Although the expression of *Shh* is diminished in the palatal epithelium of *Msx1*$^{-/-}$mice, the expression of *Gli1*, phospho-Smad1/5/8 and *Fgf7* were indistinguishable from the wild-type control (Fig. 3C,F,I).

Dlx5 inactivation rescues palatal fusion defects in *Msx1*-null mice

During palatogenesis, Shh signaling from the oral region of the palatal epithelium is required for palatal mesenchymal proliferation (Rice et al., 2004; Zhang et al., 2002). At E13.5, the expression of *Shh* in the palatal epithelium is restricted to the epithelial thickening, the developing ruga (Fig. 4A). In sagittal sections, epithelial cells that express *Shh* are not actively proliferating, whereas the mesenchymal cells underlying the *Shh*-expressing cells are actively proliferating and show a higher proliferative activity than neighboring regions of mesenchymal cells underlying non-*Shh*-expressing epithelia (Fig. 4B-D). We hypothesized that expanded Shh signaling in the absence of *Dlx5* might rescue the palatal mesenchymal proliferation defect in *Msx1*$^{-/-}$ mutant mice, a cleft palate model in which the two palatal shelves fail to meet at the midline following elevation. By comparing cell-proliferation activities in wild type, *Msx1*$^{-/-}$ and *Msx1*$^{-/-}$; *Dlx5*$^{-/-}$ palatal mesenchyme (Fig. 4E-H), we found that inactivation of *Dlx5* significantly stimulated palatal mesenchymal proliferation in the background of *Msx1*-null mutation. At E14.0, *Msx1*$^{-/-}$ mice showed significantly reduced cell proliferation (13.2±2.3%) in the palatal mesenchyme compared with the control (29.4±5.1%) (Fig. 4E,F,H). Significantly, CNC cell proliferation activity was restored (23.6±3.8%) in the palatal mesenchyme of *Msx1*$^{-/-}$; *Dlx5*$^{-/-}$ mutants (Fig. 4G,H). We did not detect altered cell proliferation activity in *Dlx5*-null mutants compared with wild-type littermates (data not shown). There was no difference in apoptotic activity in the palatal mesenchyme of wild type, *Msx1*$^{-/-}$ or *Msx1*$^{-/-}$;*Dlx5*$^{-/-}$ mutant samples (data not shown). The two palatal shelves were able to reach the midline in *Msx1*$^{-/-}$; *Dlx5*$^{-/-}$ mutants at E14.0 (Fig. 4L), probably as a consequence of the rescued palatal mesenchymal proliferation. As expected, the anterior part of the secondary palatal shelf showed insufficient expansion towards the midline in *Msx1*$^{-/-}$ mutants (Fig. 4J). The expansion of the palatal shelves in *Dlx5*$^{-/-}$ mutants was comparable to wild type (Fig. 4K,I).

To investigate whether restored cell proliferation in the palatal mesenchyme and palatal shelf extension was sufficient to restore proper palatal fusion in the *Msx1* mutant, we examined palatogenesis in *Msx1*$^{-/-}$; *Dlx5*$^{-/-}$ mice. We found that there was complete rescue of the *Msx1*$^{-/-}$ cleft palate defect in *Msx1*$^{-/-}$; *Dlx5*$^{-/-}$ mutant mice (n=15) (Fig. 5A-D). This rescued palate development required the complete absence of *Dlx5*, as *Msx1*$^{-/-}$; *Dlx5*$^{+/-}$ palates failed to fuse (data not shown). At E17.5, *Msx1*$^{-/-}$ mice showed a complete cleft of the secondary palate, the palatal shelves failed to meet at the midline (Fig. 5B,F) and the palatine processes of the maxilla and of the palatine bones were missing, leaving the vomer visible in an oral view (Fig. 5J). In the *Dlx5*$^{-/-}$ sample, fusion of the anterior palate was indistinguishable from that of the wild-type control; the soft tissue covering the anterior part of the palate was fused completely (Fig. 5C,G), and the bony parts of the hard palate were present (Fig. 5K). In *Msx1*$^{-/-}$; *Dlx5*$^{-/-}$ mutant mice, palatal fusion was rescued, with confluence of the mesenchyme and reappearance of the palatal bones that were missing in the *Msx1*$^{-/-}$ mutant (Fig. 5D,H,L).

Next, we examined whether Msx1 and Dlx5 regulate each other's expression in an upstream or downstream manner by determining if *Msx1* expression was altered in *Dlx5*$^{-/-}$ mice or vice versa. *Msx1* is expressed in the anterior part of the developing palate at E13.5. In the *Dlx5*$^{-/-}$ sample, *Msx1* expression was comparable to that of wild type (Fig. 5M,N,Q,R). A recent study failed to show that *Msx1* and *Dlx5* expression overlaps in the anterior palatal mesenchyme (Levi et al., 2006). Our data clearly demonstrate that *Dlx5* is expressed in the anterior palatal mesenchyme (Fig. 1C) and was unaffected in the *Msx1*$^{-/-}$ sample (Fig. 5O,P,S,T). Thus, Msx1 and Dlx5 do not appear to regulate each other's expression in the palate.

Rescue of cleft palate via modulation of Shh signaling

To investigate the stimulation of palatal mesenchymal cell proliferation by Shh signaling during palatogenesis, we treated E13.5 wild-type palatal explants with either BSA or Shh beads. Palatal mesenchyme cell proliferation was enhanced following Shh treatment (Fig. 6A,B insets, Fig. 6C). Moreover, ectopic Shh did not affect apoptosis in the MEE or palatal fusion (Fig. 6A-E). Explants treated with BSA or Shh beads were both able to fuse following 2

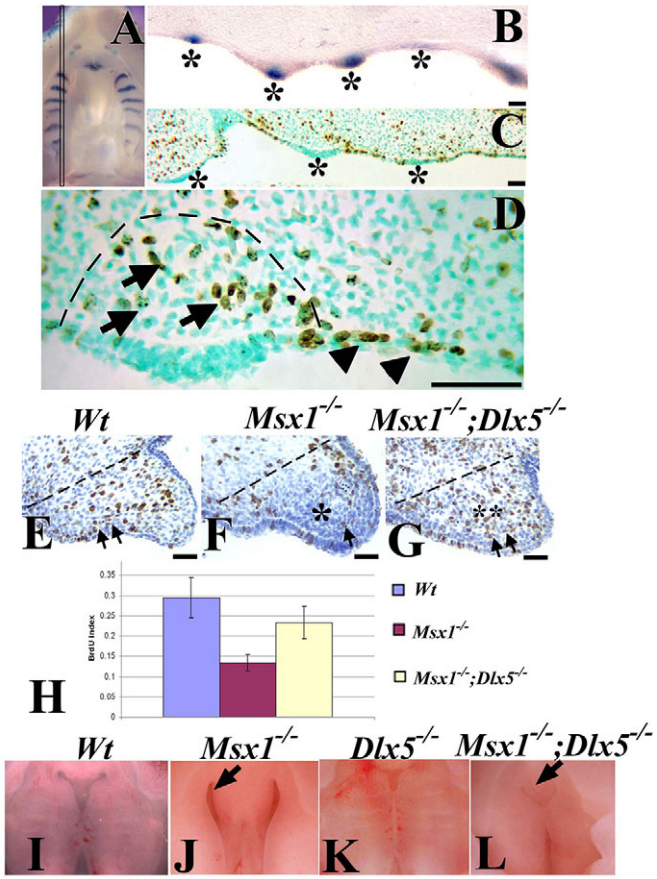

Fig. 4. Shh signaling affects palatal mesenchymal proliferation. (**A**,**B**) Whole-mount and sagittal section in situ hybridization of *Shh* in palatal epithelium at E13.5. Lines in A indicate the section plane in B. *: the expression of Shh in palatal epithelium (B). (**C**,**D**) BrdU staining of sagittal sections of E13.5 palate. Broken line: the outline of the palate and the foci of proliferating palatal mesenchymal cells (D). *: ruga where *Shh* is expressed (D). (**E-G**) BrdU staining of the anterior part of the secondary palates of E14.0 wild type (E), *Msx1*$^{-/-}$ (F), and *Msx1*$^{-/-}$; *Dlx5*$^{-/-}$ (G) embryos. Dashed lines define the area for BrdU index analyses (below dashed lines). Arrows point at BrdU-positive cells. * indicates reduced cell proliferation (F). ** indicates restored cell proliferation (G). (**H**) BrdU labeling index in wild type, *Msx1*$^{-/-}$ and *Msx1*$^{-/-}$; *Dlx5*$^{-/-}$ palatal mesenchyme. Error bars indicate 95% confidence intervals. (**I-L**) Gross appearance of palatal shelves extension at E14.5 in wild-type (I), *Msx1*$^{-/-}$ (J), *Dlx5*$^{-/-}$ (K) and *Msx1*$^{-/-}$; *Dlx5*$^{-/-}$ (L) embryos. Scale bars: 200 μm.

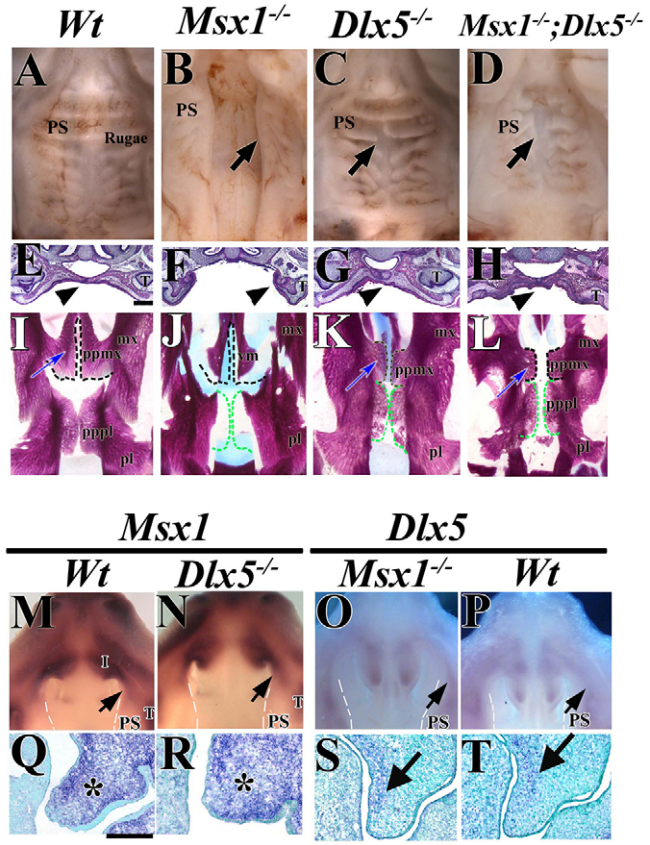

Fig. 5. *Msx1* and *Dlx5* expression in the developing palatal shelf at E13.5 and the rescue of cleft palate in *Msx1*$^{-/-}$; *Dlx5*$^{-/-}$ mice. (**A-D**) Oral view of the palate at E17.5. Arrow: the midline of palate fusion or the palatal shelf (B). (**E-H**) H and E staining of coronal sections of newborn heads. Arrowhead: palatal shelf (F) or the palate. (**I-L**) Alcian Blue and Alizarin Red staining of palates. Black broken lines: outline of maxillary palatine process. Green broken line: horizontal part of the palatine bone. Blue arrow: anterior part of the secondary palate. (**M-P**) Oral view of whole-mount in situ hybridization of *Msx1* (M, wild type; N, *Dlx5*$^{-/-}$) and *Dlx5* (O, *Msx1*$^{-/-}$; P, wild type) in the palate at E13.5. Arrow: *Msx1* or *Dlx5* expression in the palatal shelf. (**Q-T**) ISH of *Msx1* (Q, wild type; R, *Dlx5*$^{-/-}$) and *Dlx5* (S, *Msx1*$^{-/-}$; T, wild type) in coronal sections of E13.5 palate. *: *Msx1* expression. Black arrows: *Dlx5* expression domain in the nasal side of the palatal shelf. Scale bar: 200 μm. mx, maxilla; pl, palatine; ppmx, palatal process of maxilla; pppl, palatal process of palatine; PS, palate shelf; T, tooth; vm, vomer.

days of culture. Thus, increased Shh signaling has a stimulatory role on cell proliferation in the palatal mesenchyme. Furthermore, overexpressing Shh does not appear to have a major impact on the MEE cells.

To further support a role for expanded Shh signaling in the absence of *Dlx5* is responsible for the increased palatal mesenchymal cell proliferation and the rescued palatal fusion in *Msx1*$^{-/-}$; *Dlx5*$^{-/-}$ mice, we blocked Shh signaling with anti-Shh antibodies. In wild type, *Dlx5*$^{-/-}$ and *Msx1*$^{-/-}$; *Dlx5*$^{-/-}$ palatal explants, anti-Shh antibody treatment resulted in reduced mesenchymal cell proliferation activity compared with the BSA-treated explants (Fig. 6F-L). Treatment with anti-Shh antibody blocked the rescued cell proliferation in the palatal mesenchyme of *Msx1*$^{-/-}$; *Dlx5*$^{-/-}$ mice (Fig. 6H,K,L). Our data are consistent with a role for increased Shh signaling being responsible for the rescue of cell proliferation in the *Msx1*$^{-/-}$; *Dlx5*$^{-/-}$ mutant palate.

To confirm the restored mesenchymal proliferation is a result of loss of *Fgf7* expression in the nasal side of the palatal shelf, we blocked Fgf7 signaling with neutralizing antibody. In both wild type and *Msx1*$^{-/-}$ palatal explants, anti-Fgf7 antibody treatment resulted in increased mesenchymal proliferation activity compared with mouse IgG1-treated explants (Fig. 6Q). Furthermore, in *Msx1*$^{-/-}$ palatal explants treated with anti-Fgf7, the mesenchymal proliferation rate was restored to a level comparable to that of wild-type controls without anti-Fgf7 treatment (Fig. 6Q).

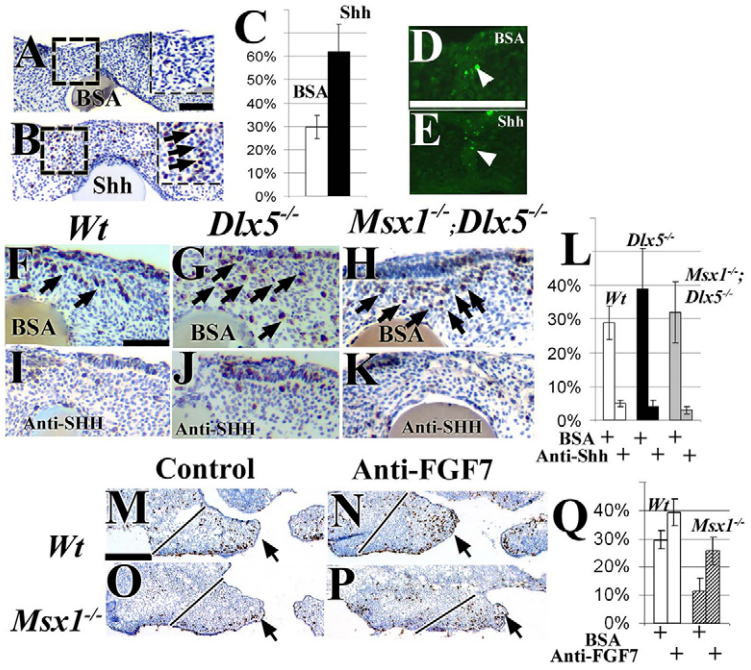

Fig. 6. Shh signaling is responsible for cell proliferation in the palate mesenchyme. (**A**,**B**) BrdU immunostaining of E13.5 wild-type palatal shelves treated with BSA or Shh beads. Insert: enlarged open box. Arrow: proliferating cells. (**C**) BrdU labeling index in BSA- and Shh-bead-treated palatal mesenchyme. Error bars indicate 95% confidence interval. (**D**,**E**) TUNEL assay of E13.5 wild-type palatal shelves treated with BSA or Shh beads. Arrowhead: apoptotic signal. (**F-K**) BrdU immunostaining of wild-type (F,I), *Dlx5*$^{-/-}$ (G,J) and *Msx1*$^{-/-}$;*Dlx5*$^{-/-}$ (H,K) palatal shelves treated with BSA (bovine serum albumin) or anti-Shh antibody (Anti-Shh). Arrows: proliferating mesenchymal cells. (**L**) BrdU index of panels F-K. (**M-P**) BrdU immunostaining (arrows) of wild type (M,O) and *Msx1*$^{-/-}$ palatal shelves treated with control mouse IgG1 or Anti-Fgf7 neutralizing antibody. (**Q**) BrdU index of M-P. Scale bars: 100 μm in A,B,D-K; 200 μm in M-P.

Msx1 and Dlx5 antagonistically regulate Shh expression to control cell proliferation in the palatal mesenchyme

The requirement for Shh signaling in the genetic rescue of cleft palate in *Msx1*$^{-/-}$; *Dlx5*$^{-/-}$ mice suggests that Shh may be regulated by both Msx1 and Dlx5. This hypothesis predicts that Shh expression should be altered as a result of null mutation of either *Msx1* or *Dlx5*. In wild-type palatal shelves at E13.5, *Shh* expression was restricted to the oral side of the palatal epithelium and limited to defined stripes that correspond to the developing rugae (Fig. 7A, Fig. 2I, Fig. 4B). In the epithelial cells covering the palatal shelf of *Msx1*$^{-/-}$ mice, Shh expression was not detectable (Fig. 7B, Fig. 2O). Loss of *Dlx5* resulted in expanded *Shh* expression in the palatal epithelium (Fig. 7C, Fig. 2J). This medial expansion of Shh signaling suggests that Dlx5 was required to suppress *Shh* expression in the palate. We also detected a similar expansion of *Shh* expression in the palatal epithelium of *Msx1*$^{-/-}$; *Dlx5*$^{-/-}$ mutant mice (Fig. 7D). Thus, expanded Shh expression is independent of Msx1 signaling in the *Dlx5* mutant. *Gli1* is a mediator and target for the Shh pathway that enables us to detect Shh-responsive cells. We found that *Gli1* was expressed in the oral half of wild-type palatal mesenchyme adjacent to the epithelium where *Shh* was expressed (Fig. 1G-I, Fig. 3A). In *Dlx5*$^{-/-}$ palate, *Gli1* expression expanded into the nasal half of the palatal shelf (see Fig. 3B) corresponding to the expansion in *Shh* expression (Fig. 7C). In *Msx1*$^{-/-}$ palate, however, *Gli1* expression remained restricted to the oral half of the palate (Fig. 3C). Therefore, we conclude that Msx1 and Dlx5 antagonistically regulate *Shh* expression in the palatal epithelium; however, the capacity of palatal mesenchyme to respond to Shh signaling is independent of Msx1 status.

The expansion of *Shh* expression into the nasal side of the palatal epithelium in *Dlx5*$^{-/-}$ mice suggests that Dlx5 is required for restricting *Shh* expression to the oral side of the palatal epithelium. However, *Shh* is expressed in the oral side of the palatal epithelium (Fig. 1G), whereas *Dlx5* is expressed in the nasal side of the palatal mesenchyme (Fig. 1C). This spatial relationship and the fact that Dlx5 functions as a transcription factor suggest that a Dlx5 downstream target gene in the palatal mesenchyme mediates the restriction of *Shh* expression. Endogenous *Fgf7* is expressed in the nasal half of the palatal mesenchyme (Dlx5-expressing domain), whereas *Shh* is absent from the corresponding palatal epithelium (Fig. 1C,D,G). In the *Dlx5* mutant, *Fgf7* expression is specifically diminished in the nasal half of the palatal mesenchyme but *Fgf7* expression in the craniobase persists (Fig. 3H), suggesting that Dlx5 is required for *Fgf7* expression in the nasal half of the palatal mesenchyme. Fgf7 has previously been shown to inhibit Shh signaling during lung and limb development (Bellusci et al., 1997; Yonei-Tamura et al., 1999). To test if Fgf7 can inhibit Shh expression in the palatal epithelium, we placed Fgf7 beads into E13.5 palatal shelves in vitro and analyzed *Shh* expression. After 1 day of culture in serumless, chemically defined media, Fgf7-bead-treated samples showed a dramatic reduction of *Shh* expression in the palatal epithelium compared with BSA-treated samples (Fig. 7E,F). Furthermore, Fgf7 beads were able to inhibit *Shh* expression in the palatal epithelium of *Dlx5*$^{-/-}$ samples (Fig. 7G), suggesting that Dlx5-dependent Fgf7 expression is sufficient to inhibit the expression of *Shh* in the nasal half of palatal epithelium during palatogenesis. To confirm the inhibitory effect of Fgf7 on *Shh* expression, we then treated wild type and *Msx1*$^{-/-}$ palatal explants with anti-Fgf7 neutralizing antibody. Inhibition of Fgf7 signaling enhanced *Shh* expression in both wild type and *Msx1* mutant mice (Fig. 7I,K) and restored *Shh* expression in the anterior region of the palatal shelf (Fig. 7K). Interestingly, exogenous Shh repressed *Fgf7* expression (Fig. 7L-N), suggesting a feedback loop in Fgf7/Shh signaling interaction in regulating palatogenesis.

Dlx5 is crucial for patterning the soft palate

In the posterior part of the palate, we discovered additional defects with complete phenotype penetrance in *Dlx5*$^{-/-}$ mice. These included a shortened, detached soft palate and the presence of a uvula-like structure (Fig. 8B). Wild-type mice have a soft palate with a posterior border attached to the pharyngeal wall (Fig. 8A,C). The shortened soft palate in *Dlx5*$^{-/-}$ mice resembles velopharyngeal insufficiency and fails to provide an adequate seal between the nasal

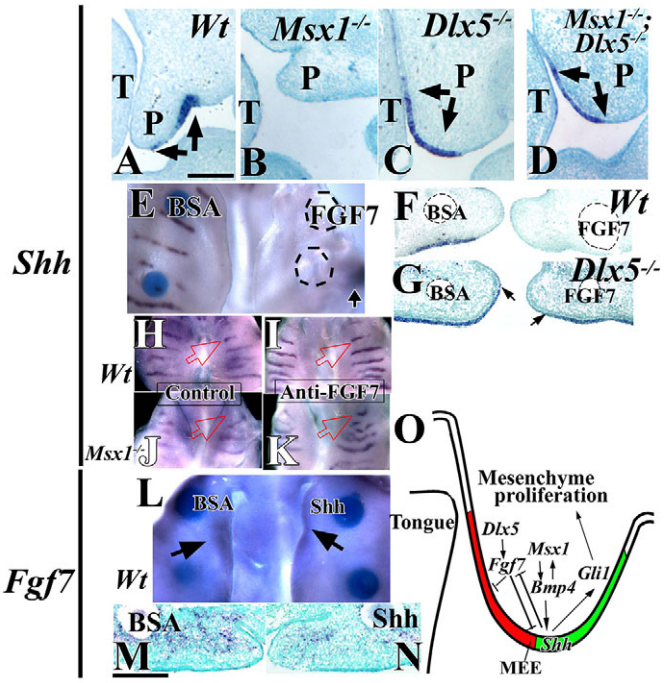

Fig. 7. Regulation of Shh signaling in the developing palate. (**A-D**) In situ hybridization (ISH) of coronal sections of E13.5 mouse embryos, showing *Shh* expression in the palatal epithelium. (**E**) Whole-mount ISH of *Shh* in wild-type palatal explants treated with BSA beads (blue) and Fgf7 beads (white). Arrow: the expression of *Shh* in the tooth bud served as control. (**F**,**G**) ISH of *Shh* in coronal sections of palatal explants treated with BSA and Fgf7 beads. (**H-K**) Oral view of whole-mount ISH of *Shh* in palatal explants treated with IgG1 (H, wild type; J, *Msx1*$^{-/-}$) or anti-Fgf7 neutralizing antibody (I, wild type; K, *Msx1*$^{-/-}$). (**L**) Oral view of whole-mount ISH analysis of *Fgf7* expression (arrows) in palatal explants treated with BSA beads and Shh beads. (**M**,**N**) ISH analysis of *Fgf7* expression in coronal sections of palatal explants treated with BSA and Shh beads. (**O**) Schematic drawing depicting the antagonistic regulation of Msx1 and Dlx5 on *Shh* expression to control mesenchymal cell proliferation during palatogenesis. P, palate; T, tongue. Scale bars: 200 μm.

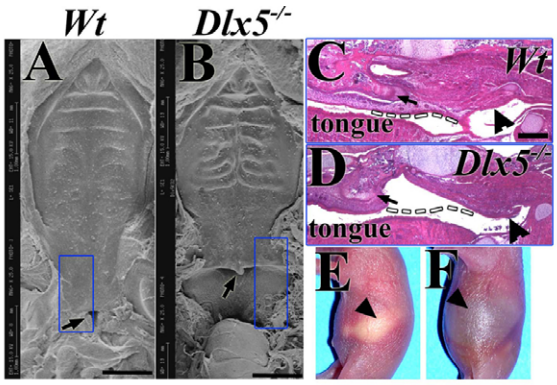

Fig. 8. Soft palate patterning defects in *Dlx5*$^{-/-}$ newborn mice. (**A**,**B**) SEM of newborn wild-type and *Dlx5*$^{-/-}$ mice heads (oral view). Arrow in A: the attachment of the posterior palate to the posterior pharyngeal wall. Arrow in B: the uvula-like structure in *Dlx5*$^{-/-}$. Blue box: sagittal section of the posterior soft palate shown in C and D. (**C**,**D**) Sagittal section of newborn head. Arrow: posterior border of the soft palate. Broken line shows normal soft palate in C and shortening of soft palate in *Dlx5*$^{-/-}$ mice (D). (**E**,**F**) Excessive air retention in the stomach of *Dlx5*$^{-/-}$ newborn mice. *Wt*: wild type. Scale bars: 1 mm.

and oral pharynx (Fig. 8B,D). This anatomical defect also appears to cause air to enter the gastrointestinal tract, as the stomachs of all *Dlx5*$^{-/-}$ newborns were inflated with air (Fig. 8E,F).

DISCUSSION

Oronasal patterning of the palatal shelf

In this study, we report the existence of O-N patterning and its molecular regulation in the developing palatal shelf. Specifically, phospho-Smad1/5/8 antibody staining marks the activation of BMP signaling and appears to be restricted to the nasal side of the palatal mesenchyme. Interestingly, the expression of *Bmp4* and *Bmp2* is uniform throughout the palatal mesenchyme (Zhang et al., 2002). The expression of other members of the BMP and GDF families has not been thoroughly investigated. The functional significance of Bmpr1 has been demonstrated in a recent study, in which conditional inactivation of *Bmpr1a* in the CNC-derived mesenchyme results in cleft lip and palate (Liu et al., 2005). However, the distribution of *Bmpr1a* in the palatal mesenchyme still needs to be investigated in order to provide an explanation for the asymmetrical activation of BMP signaling in the palatal mesenchyme. It remains possible that the regional differential expression of Bmp receptor controls the establishment of the BMP-responsive domain in the palatal mesenchyme. Alternatively, it is plausible that there is an inhibition of BMP signaling activation on the oral side of the palatal mesenchyme. Further analysis will elucidate the molecular mechanism that controls the asymmetrical activation of BMP signaling in the palate that ultimately results in the formation of palatal bone towards the nasal side of the palate. Significantly, our study demonstrates that, although the palatal mesenchyme is populated with CNC-derived cells, they are not a homogenous population and need to be evaluated and distinguished by molecular marker analysis. This insight will guide our approach in the evaluation of the CNC-derived palatal mesenchyme during palatogenesis.

The restricted expression of *Dlx5* on the nasal side and the expansion of the oral side growth of *Dlx5*$^{-/-}$ palate clearly suggest that Dlx5 actively participates in the O-N patterning of the developing palate. By contrast, loss of *Msx1* does not alter the O-N patterning of the palate. Thus, we conclude that Msx1 is not involved in the O-N patterning of the palate.

Fgf7 is expressed in the nasal region of the palatal mesenchyme and exogenous Fgf7 beads inhibit the expression of *Shh* in the nasal region of the palatal epithelium, strongly suggesting that Fgf7 is a member of the hierarchy that determines O-N patterning of the palatal mesenchyme. The null mutation of *Fgf7* in mice did not generate an obvious palatal phenotype (Guo et al., 1996), as is also the case for the majority of *Dlx5*$^{-/-}$ mice (Depew et al., 1999).

The restricted expression of *Shh* in the oral side of the palatal epithelium and of *Gli1* and *Fgf10* in the oral side of the palatal mesenchyme suggests that Shh signaling is crucial for the development of the oral side of the palate. In the developing palatal shelf, the cell-surface receptors for Shh (*Ptch*1 and *Smo*), hedgehog signaling inhibitors (*Hhip1* and *Gas1*), and Hh-signaling mediator (*Gli*-family zinc-finger transcription factors) are expressed in the palatal epithelium and mesenchyme (Rice et al., 2006). Conditional inactivation of *Shh* in the epithelium results in dramatic shortening of the palatal shelves and a wide cleft palate, whereas conditional inactivation of *Smo* in the epithelium does not disrupt palatogenesis

(Hilliard et al., 2005), consistent with the model that the underlying palatal mesenchyme is the recipient of Shh signals. Furthermore, mutations in *Gli2* or *Gli3* cause facial abnormalities including cleft palate (Mo et al., 1997). We conclude that it is likely that the restricted expression of Shh in the palate is the result of the patterning, in contrast to the setting in the spinal cord, where Shh functions as an inductive signal of patterning. *Gli1*, which marks the Shh-responding cells (Hooper and Scott, 2005; Lum and Beachy, 2004), is a stronger candidate for the molecule responsible for the patterning of the oral side palatal mesenchyme, because its expression is restricted to the oral half of the palate (see Fig. 3). Our results suggest that, although Shh is not involved in the O-N patterning of the palatal shelf, Shh responsiveness determines the oral half of the palate.

The persistence of *Gli1* expression in *Msx1*$^{-/-}$ palates indicates that the *Gli1* expression in the oral side of the palatal mesenchyme does not require the presence of Shh and is not under the regulation of Msx1. Interestingly, a recent study shows that *Gli1* and *Ptch1* expression are downregulated in the palatal mesenchyme following the ectoderm-specific inactivation of *Shh* gene (Lan and Jiang, 2009). To date, studies have shown that hedgehog and TGF-β signaling induces *Gli1* expression, whereas Snail/Slug, and Notch signaling, inhibits *Gli1* expression (Katoh and Katoh, 2009). Further analysis is necessary to reveal the comprehensive regulation of *Gli1* expression during palatogenesis.

The function of Shh signaling in palatal fusion

Previous studies have shown that Shh functions as a crucial mitogenic factor for the palate mesenchyme through its coordination of Fgf10-Fgfr2b and Msx1-Bmp4 signaling networks (Rice et al., 2004; Zhang et al., 2002). We have shown here that the actively proliferating palatal mesenchymal cells are those adjacent to the *Shh*-expressing epithelial cells. This spatial correlation is consistent with the restricted range of Shh activity in the limb bud (Li et al., 2006). Shh beads are able to stimulate mesenchymal proliferation in palate explants in vitro, and mesenchymal cell proliferation is reduced in palate explants treated with anti-Shh antibody. In *Dlx5*$^{-/-}$ palates, expanded Shh signaling and increased cell proliferation in the palatal mesenchyme might contribute to the overgrowth of rugae and eventual folding of the palatal shelf. However, compromised *Shh* expression is accompanied by a reduction in cell proliferation in both palatal mesenchyme and epithelium in *Fgf10*$^{-/-}$ mice (Rice et al., 2004).

Previous studies have shown that the Shh signaling cascade is regulated at multiple levels. Cholesterol modification can restrict the spread of Shh and control the range and shape of the Shh morphogen gradient (Li et al., 2006). At the intracellular level, the combined activities of hedgehog signaling inhibitors (*Hhip* and *Ptch1*) are crucial for tightly controlled Shh activity during pancreas development (Kawahira et al., 2003) and during the initiation of tooth development (Cobourne et al., 2004). Another important mechanism affecting Shh signaling is tissue-tissue interaction. A previous study shows that Msx1 controls the expression of *Bmp4*, which in turn positively regulates *Shh* expression during palatogenesis (Zhang et al., 2002). Fgf10 positively regulates *Shh* expression through Fgfr2b in the palatal epithelium (Rice et al., 2004). We have shown in this study that transcriptional antagonism between Msx1 and Dlx5 in regulating Shh expression ensures the precise spatiotemporal control of Shh signaling during palatal shelf development. More specifically, Msx1-mediated BMP4 signaling is responsible for inducing Shh signaling in the palatal epithelium, whereas Dlx5 is responsible for the indirect inhibition of Shh signaling in the nasal side of the palatal epithelium. As the result of this antagonistic control, there is an asymmetrical distribution of Shh signaling in the palatal epithelium. This specific Shh expression pattern is crucial for the growth and elevation of palatal shelf before fusion.

Shh as a potential target for repairing a specific group of cleft palate cases

We propose that Shh signaling is a potential target for the repair of the group of cleft palate cases that result from the failure of palatal shelves to meet at the midline due to compromised palatal mesenchymal proliferation. Restored Shh expression in the palatal epithelium of *Msx1*$^{-/-}$*; Dlx5*$^{-/-}$ mice is sufficient to trigger the Shh signaling cascade leading to palatal mesenchyme proliferation and fusion, supported by the evidence that inhibition of Shh signaling in *Msx1*$^{-/-}$*; Dlx5*$^{-/-}$ mice reverses the rescue of palatal mesenchyme proliferation. Furthermore, Shh is the converging point for Bmp signaling and Fgf signaling during the expansion stage of palatogenesis (Rice et al., 2004; Zhang et al., 2002). Taking these findings together, we conclude that modulating Shh signaling may provide an opportunity to direct palatal shelf growth and rescue palatal fusion in mutant models with insufficient palatal shelf growth and cleft palate defect.

Dlx5 and soft palate development

The discovery of a soft palate defect in *Dlx5*$^{-/-}$ mice may have significant implications from an evolutionary perspective. Unlike humans, mice have a soft palate that is attached to the posterior pharyngeal wall. The epiglottis is above the level of soft palate; mice can therefore suckle and breathe at the same time. In humans, the posterior border of the soft palate is free and the epiglottis is below the posterior border of soft palate. This anatomical feature is an important advancement in human evolution because proper function of the soft palate is crucial for speech development. Furthermore, soft palate, along with epiglottis and soft tissue structures within the larynx, acts as a valve to prevent food and liquid from entering lower parts of the respiratory tract. We have found that loss of *Dlx5* results in a shortened soft palate in mice. Because *Dlx* genes are known for their function in regulating the identity of craniofacial structures and morphological novelty in the vertebrate lineage (Beverdam et al., 2002; Depew et al., 2002; Neidert et al., 2001), our data suggest that Dlx5 plays an important role in patterning the proximal region of the pharyngeal arch derivatives.

Interaction of Msx and Dlx signaling

Our data clearly demonstrate that Msx1 and Dlx5 operate in parallel in regulating downstream target gene expression during palatogenesis. Recent studies show that the function of *Msx* genes is to control CNC cell cycle progression, as loss of both *Msx1* and *Msx2* genes results in defects in CNC cell proliferation and survival but does not affect the expression of *Dlx5* and the patterning of the branchial arch (Han et al., 2003; Ishii et al., 2005). However, members of the *Dlx* gene family mainly control the patterning of the craniofacial skeleton, as loss of both *Dlx5* and *Dlx6* genes results in homeotic transformation of the lower jaw to upper jaw (Depew et al., 2002). Interestingly, the expression of *Msx1* and *Msx2* is reduced in the first branchial arch of the *Dlx5; Dlx6* compound mutant samples, suggesting that *Msx* genes may function downstream of Dlx5 and Dlx6 in regulating the patterning of the branchial arch derivatives (Depew et al., 2002). In tooth development, however, *Msx1* is required for *Dlx5* expression in the dental mesenchyme. *Msx1* and *Dlx5* appear to work synergistically to regulate tooth and alveolar bone development (Zhang et al., 2003). Clearly, Msx1 and

Dlx5 can work either antagonistically or synergistically to regulate downstream target gene expression, depending on the context. The outcome of this interaction and whether Msx1 and Dlx5 work in parallel or in a sequential manner depends on the cell and tissue type where the interaction takes place. This operating logic allows for diverse outcomes associated with Msx1/Dlx5 interaction in regulating organogenesis. Equally important, perturbation of the Msx1/Dlx5 interaction may affect an array of downstream target genes and sets the stage for dysmorphogenesis.

Acknowledgements
We thank Henry Sucov for critical reading and comments. This study was support by grants from the NIDCD, NIH (R01 DC005667) to John Rubenstein and the National Institute of Dental and Craniofacial Research, NIH (DE012711 and DE014078) to Yang Chai. Deposited in PMC for release after 12 months.

Supplementary material
Supplementary material for this article is available at
http://dev.biologists.org/cgi/content/full/136/24/4225/DC1

References

Bei, M., Kratochwil, K. and Maas, R. L. (2000). BMP4 rescues a non-cell-autonomous function of Msx1 in tooth development. *Development* **127**, 4711-4718.
Bellusci, S., Grindley, J., Emoto, H., Itoh, N. and Hogan, B. L. (1997). Fibroblast growth factor 10 (FGF10) and branching morphogenesis in the embryonic mouse lung. *Development* **124**, 4867-4878.
Beverdam, A., Merlo, G. R., Paleari, L., Mantero, S., Genova, F., Barbieri, O., Janvier, P. and Levi, G. (2002). Jaw transformation with gain of symmetry after Dlx5/Dlx6 inactivation: mirror of the past? *Genesis* **34**, 221-227.
Chai, Y. and Maxson, R. E., Jr (2006). Recent advances in craniofacial morphogenesis. *Dev. Dyn.* **235**, 2353-2375.
Cobourne, M. T., Miletich, I. and Sharpe, P. T. (2004). Restriction of sonic hedgehog signalling during early tooth development. *Development* **131**, 2875-2885.
Cobourne, M. T., Xavier, G. M., Depew, M., Hagan, L., Sealby, J., Webster, Z. and Sharpe, P. T. (2009). Sonic hedgehog signalling inhibits palatogenesis and arrests tooth development in a mouse model of the nevoid basal cell carcinoma syndrome. *Dev. Biol.* **331**, 38-49.
Depew, M. J., Liu, J. K., Long, J. E., Presley, R., Meneses, J. J., Pedersen, R. A. and Rubenstein, J. L. (1999). Dlx5 regulates regional development of the branchial arches and sensory capsules. *Development* **126**, 3831-3846.
Depew, M. J., Lufkin, T. and Rubenstein, J. L. (2002). Specification of jaw subdivisions by Dlx genes. *Science* **298**, 381-385.
Ferguson, M. W. (1988). Palate development. *Development* **103 Suppl.**, 41-60.
Guo, L., Degenstein, L. and Fuchs, E. (1996). Keratinocyte growth factor is required for hair development but not for wound healing. *Genes Dev.* **10**, 165-175.
Han, J., Ito, Y., Yeo, J. Y., Sucov, H. M., Maas, R. and Chai, Y. (2003). Cranial neural crest-derived mesenchymal proliferation is regulated by Msx1-mediated p19(INK4d) expression during odontogenesis. *Dev. Biol.* **261**, 183-196.
Hilliard, S. A., Yu, L., Gu, S., Zhang, Z. and Chen, Y. P. (2005). Regional regulation of palatal growth and patterning along the anterior-posterior axis in mice. *J. Anat.* **207**, 655-667.
Hooper, J. E. and Scott, M. P. (2005). Communicating with Hedgehogs. *Nat. Rev. Mol. Cell Biol.* **6**, 306-317.
Hu, G., Vastardis, H., Bendall, A. J., Wang, Z., Logan, M., Zhang, H., Nelson, C., Stein, S., Greenfield, N., Seidman, C. E. et al. (1998). Haploinsufficiency of MSX1: a mechanism for selective tooth agenesis. *Mol. Cell. Biol.* **18**, 6044-6051.
Ishii, M., Han, J., Yen, H. Y., Sucov, H. M., Chai, Y. and Maxson, R. E., Jr (2005). Combined deficiencies of Msx1 and Msx2 cause impaired patterning and survival of the cranial neural crest. *Development* **132**, 4937-4950.
Ito, Y., Yeo, J. Y., Chytil, A., Han, J., Bringas, P., Jr, Nakajima, A., Shuler, C. F., Moses, H. L. and Chai, Y. (2003). Conditional inactivation of Tgfbr2 in cranial neural crest causes cleft palate and calvaria defects. *Development* **130**, 5269-5280.
Jeong, J., Mao, J., Tenzen, T., Kottmann, A. H. and McMahon, A. P. (2004). Hedgehog signaling in the neural crest cells regulates the patterning and growth of facial primordia. *Genes Dev.* **18**, 937-951.
Jessell, T. M. (2000). Neuronal specification in the spinal cord: inductive signals and transcriptional codes. *Nat. Rev. Genet.* **1**, 20-29.
Jumlongras, D., Bei, M., Stimson, J. M., Wang, W. F., DePalma, S. R., Seidman, C. E., Felbor, U., Maas, R., Seidman, J. G. and Olsen, B. R. (2001). A nonsense mutation in MSX1 causes Witkop syndrome. *Am. J. Hum. Genet.* **69**, 67-74.
Katoh, Y. and Katoh, M. (2009). Integrative genomic analyses on GLI1: Positive regulation of GLI1 by Hedgehog-GLI, TGFbeta-Smads, and RTK-PI3K-AKT signals, and negative regulation of GLI1 by Notch-CSL-HES/HEY, and GPCR-Gs-PKA signals. *Int. J. Oncol.* **35**, 187-192.
Kawahira, H., Ma, N. H., Tzanakakis, E. S., McMahon, A. P., Chuang, P. T. and Hebrok, M. (2003). Combined activities of hedgehog signaling inhibitors regulate pancreas development. *Development* **130**, 4871-4879.
Lan, Y. and Jiang, R. (2009). Sonic hedgehog signaling regulates reciprocal epithelial-mesenchymal interactions controlling palatal outgrowth. *Development* **136**, 1387-1396.
Levi, G., Mantero, S., Barbieri, O., Cantatore, D., Paleari, L., Beverdam, A., Genova, F., Robert, B. and Merlo, G. R. (2006). Msx1 and Dlx5 act independently in development of craniofacial skeleton, but converge on the regulation of Bmp signaling in palate formation. *Mech. Dev.* **123**, 3-16.
Li, Y., Zhang, H., Litingtung, Y. and Chiang, C. (2006). Cholesterol modification restricts the spread of Shh gradient in the limb bud. *Proc. Natl. Acad. Sci. USA* **103**, 6548-6553.
Liu, W., Sun, X., Braut, A., Mishina, Y., Behringer, R. R., Mina, M. and Martin, J. F. (2005). Distinct functions for Bmp signaling in lip and palate fusion in mice. *Development* **132**, 1453-1461.
Lum, L. and Beachy, P. A. (2004). The Hedgehog response network: sensors, switches, and routers. *Science* **304**, 1755-1759.
Martinez-Alvarez, C., Tudela, C., Perez-Miguelsanz, J., O'Kane, S., Puerta, J. and Ferguson, M. W. (2000). Medial edge epithelial cell fate during palatal fusion. *Dev. Biol.* **220**, 343-357.
Mo, R., Freer, A. M., Zinyk, D. L., Crackower, M. A., Michaud, J., Heng, H. H., Chik, K. W., Shi, X. M., Tsui, L. C., Cheng, S. H. et al. (1997). Specific and redundant functions of Gli2 and Gli3 zinc finger genes in skeletal patterning and development. *Development* **124**, 113-123.
Neidert, A. H., Virupannavar, V., Hooker, G. W. and Langeland, J. A. (2001). Lamprey Dlx genes and early vertebrate evolution. *Proc. Natl. Acad. Sci. USA* **98**, 1665-1670.
Qiu, M., Bulfone, A., Ghattas, I., Meneses, J. J., Christensen, L., Sharpe, P. T., Presley, R., Pedersen, R. A. and Rubenstein, J. L. (1997). Role of the Dlx homeobox genes in proximodistal patterning of the branchial arches: mutations of Dlx-1, Dlx-2, and Dlx-1 and -2 alter morphogenesis of proximal skeletal and soft tissue structures derived from the first and second arches. *Dev. Biol.* **185**, 165-184.
Rice, R., Spencer-Dene, B., Connor, E. C., Gritli-Linde, A., McMahon, A. P., Dickson, C., Thesleff, I. and Rice, D. P. (2004). Disruption of Fgf10/Fgfr2b-coordinated epithelial-mesenchymal interactions causes cleft palate. *J. Clin. Invest.* **113**, 1692-1700.
Rice, R., Connor, E. and Rice, D. P. (2006). Expression patterns of Hedgehog signalling pathway members during mouse palate development. *Gene Expr. Patterns* **6**, 206-212.
Satokata, I. and Maas, R. (1994). Msx1 deficient mice exhibit cleft palate and abnormalities of craniofacial and tooth development. *Nat. Genet.* **6**, 348-356.
Shuler, C. F. (1995). Programmed cell death and cell transformation in craniofacial development. *Crit. Rev. Oral Biol. Med.* **6**, 202-217.
van den Boogaard, M. J., Dorland, M., Beemer, F. A. and van Amstel, H. K. (2000). MSX1 mutation is associated with orofacial clefting and tooth agenesis in humans. *Nat. Genet.* **24**, 342-343.
Vastardis, H., Karimbux, N., Guthua, S. W., Seidman, J. G. and Seidman, C. E. (1996). A human MSX1 homeodomain missense mutation causes selective tooth agenesis. *Nat. Genet.* **13**, 417-421.
Vaziri Sani, F., Hallberg, K., Harfe, B. D., McMahon, A. P., Linde, A. and Gritli-Linde, A. (2005). Fate-mapping of the epithelial seam during palatal fusion rules out epithelial-mesenchymal transformation. *Dev. Biol.* **285**, 490-495.
Washington Smoak, I., Byrd, N. A., Abu-Issa, R., Goddeeris, M. M., Anderson, R., Morris, J., Yamamura, K., Klingensmith, J. and Meyers, E. N. (2005). Sonic hedgehog is required for cardiac outflow tract and neural crest cell development. *Dev. Biol.* **283**, 357-372.
Xu, X., Bringas, P., Jr, Soriano, P. and Chai, Y. (2005). PDGFR-alpha signaling is critical for tooth cusp and palate morphogenesis. *Dev. Dyn.* **232**, 75-84.
Yang, L., Zhang, H., Hu, G., Wang, H., Abate-Shen, C. and Shen, M. M. (1998). An early phase of embryonic Dlx5 expression defines the rostral boundary of the neural plate. *J. Neurosci.* **18**, 8322-8330.
Yonei-Tamura, S., Endo, T., Yajima, H., Ohuchi, H., Ide, H. and Tamura, K. (1999). FGF7 and FGF10 directly induce the apical ectodermal ridge in chick embryos. *Dev. Biol.* **211**, 133-143.
Zhang, Z., Song, Y., Zhao, X., Zhang, X., Fermin, C. and Chen, Y. (2002). Rescue of cleft palate in Msx1-deficient mice by transgenic Bmp4 reveals a network of BMP and Shh signaling in the regulation of mammalian palatogenesis. *Development* **129**, 4135-41346.
Zhang, Z., Song, Y., Zhang, X., Tang, J., Chen, J. and Chen, Y. (2003). Msx1/Bmp4 genetic pathway regulates mammalian alveolar bone formation via induction of Dlx5 and Cbfa1. *Mech. Dev.* **120**, 1469-1479.